

Nanoscale ductile grinding of glass by diamond fibres

P. G. PARTRIDGE, A. J. FOOKES, E. D. NICHOLSON*, T. PEARCE†, G. MEADEN
*Interface Analysis Centre, *Institute of Grinding Technology, School of Chemistry, and †University of Bristol, Bristol, UK*

Chemical vapour-deposited diamond fibres have been used to grind soda glass. The surface topography was studied using scanning electron microscopy and atomic force microscopy techniques. The diamond surface facets and edges led to grinding without surface cracking and to surface roughness, R_a , values in the range 3–50 nm. The grinding mechanism involved the formation by ductile flow of glass ribbons adjacent to the grinding grooves. This grinding mechanism was similar to that reported for single-point diamond machining. The potential for ductile grinding with diamond fibres is discussed.

1. Introduction

Diamond in the form of natural or high-pressure synthesized particles is a superabrasive material used for grinding, polishing, drilling and precision machining the hardest materials, such as hypereutectic Al–Si alloys, bulk ceramics and plasma-sprayed coatings [1,2]. Thin diamond films produced by chemical vapour deposition (CVD) can have properties almost identical to those reported for natural diamond, e.g. values of Young's modulus, thermal conductivity, hardness and wear resistance greater than that of any other material, together with low values for density and friction coefficient [3]. Without the cost and size limitation imposed by particulate diamond, a major market is predicted for CVD diamond coatings as an abrasive material [4]. Recently diamond fibres have been manufactured by CVD on to tungsten wires and ceramic fibres [3,5]. The fibres may be used to reinforce polymer, metal or ceramic matrices [5,6,7]. These high stiffness composites may be useful for ductile grinding. In this process, brittle materials are ground in a ductile manner without cracking by removing material on a sub-micrometre scale, using diamond-particle impregnated diamond wheels. Various materials have been successfully ground under these conditions, such as optical glass and glass ceramics [8–10], fused silica [11], alumina, silicon nitride, silicon carbide [10,12], Mn–Zn ferrite [13] and silicon [10]. Ductile-mode grinding offers the possibility of reducing the surface defect size to increase the mechanical properties of ceramics and of avoiding or reducing the cost of polishing optical materials. A preliminary investigation into the grinding of soda glass by single CVD diamond fibres has been carried out. The results obtained are described in this paper and compared with data for conventional line and single-point diamond grinding.

2. Experimental procedure

Diamond fibres, $\sim 100 \mu\text{m}$ diameter (Fig. 1a), were produced by CVD of diamond films, $\sim 25\text{--}40 \mu\text{m}$ thick, on to $25 \mu\text{m}$ diameter tungsten wire in a hot filament reactor, as described elsewhere [3]. The diamond film consisted of long columnar grains oriented in the radial direction around the fibre axis, with a typical texture [14] that led to (100) and (111) crystal facets and diamond edges and points on the cylindrical surface of the fibre (Fig. 1b). With a diamond grain diameter at the surface of $\sim 5 \mu\text{m}$, the number of edges and points on the fibre surface was about 10^4mm^{-2} . Grinding was carried out using single fibres of length $L_F = 5 \text{mm}$ and the as-deposited cylindrical fibre surface (Fig. 2). A fibre was embedded in resin to a depth of about the half the fibre diameter and attached to a balanced arm in contact with a glass disc rotating at 25 r.p.m. in a simple pin-on-disc machine. A weight of 200 g placed on the arm applied a normal force of $\sim 2 \text{N}$ on the fibre. The soda glass samples were $50 \text{mm} \times 4 \text{mm}$ discs and the wear track radius dictated the surface speed of 0.05m s^{-1} . All grinding was carried out in air without lubricant.

The fibre axis was oriented normal to the grinding direction. Under low loads and small depths of cut, typical of ductile grinding conditions, only the highest diamond facets initially made contact with the glass. The 5 mm long fibres became very slightly bent convex towards the glass surface during embedding in the resin. Consequently, the grinding track was only about 1 and 2 mm wide after one and ten revolutions, respectively, of the glass work piece. The track was composed of individual grooves made by the highest diamond facets. With increasing number of revolutions or load, the depth of cut increased and more facets made contact with the surface. Eventually the grooves covered the whole width of the track and the

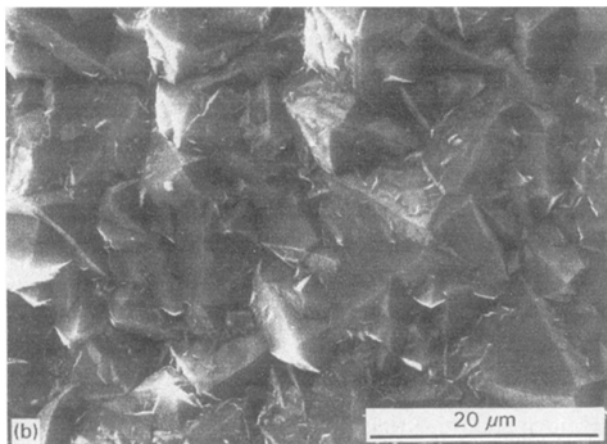
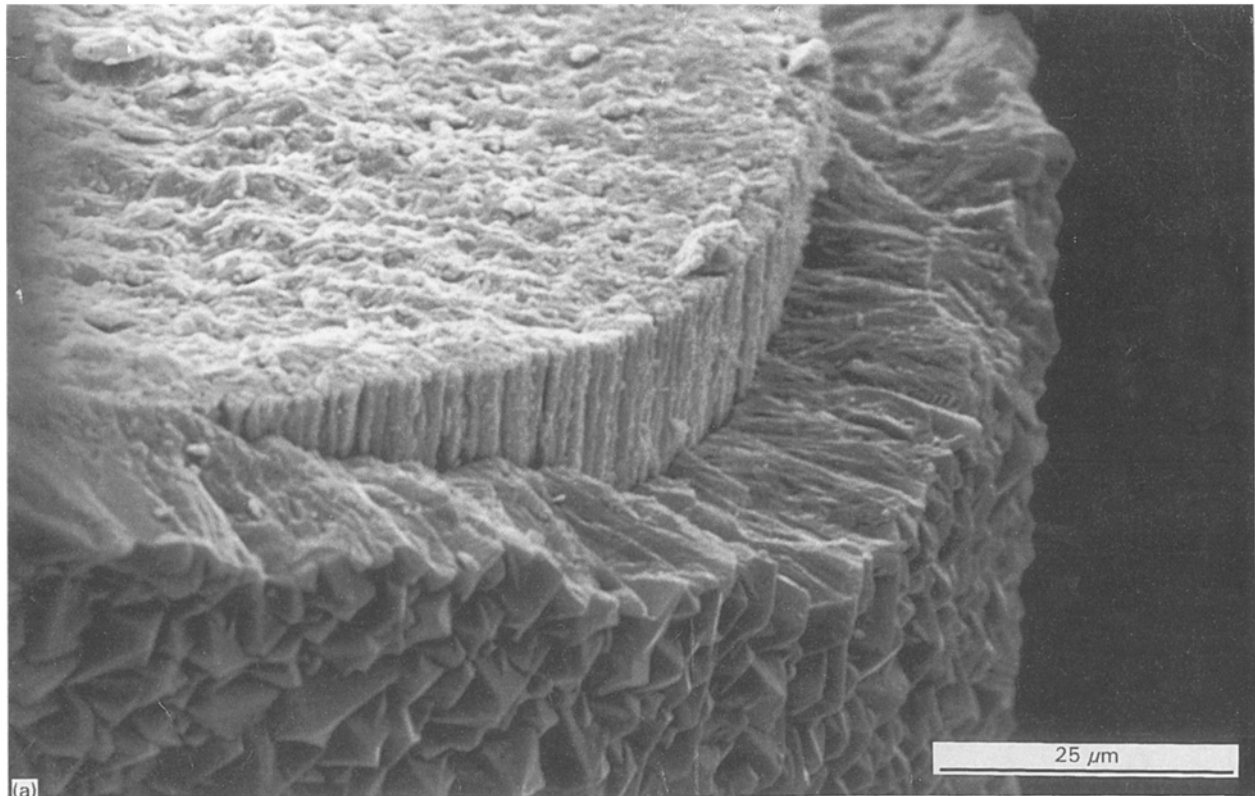


Figure 1 Diamond fibre surfaces. (a) Diamond fibre with tungsten core showing columnar grains in the fractured end face and faceted cylindrical surface. (b) Surface showing diamond facets, points and edges.

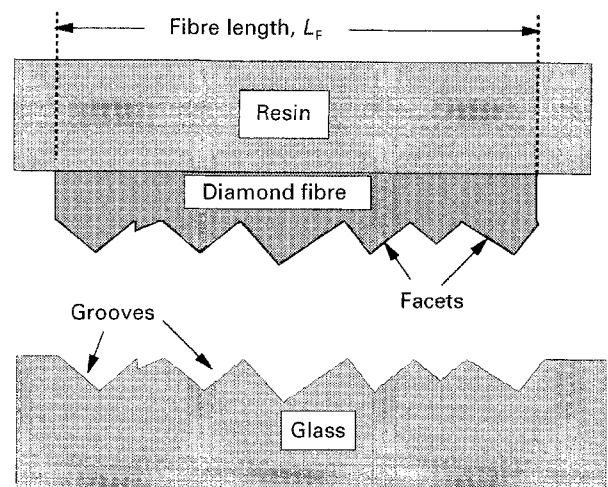


Figure 2 Schematic drawing of a vertical section, normal to the grinding direction and through a resin-mounted diamond fibre and glass surface, showing the shape of grooves made by facets.

track width equalled the fibre length, as shown schematically in Fig. 2.

The ground surface was characterized by optical and scanning electron microscopy (SEM), and atomic force microscopy (AFM). The diamond fibres were examined before and after grinding by SEM and Raman spectroscopy.

3. Results

3.1. Surface topography

A part of a 200 g 5 mm ground track after ten revolutions is shown after ultrasonic cleaning in the optical micrograph in Fig. 3; the total grinding distance was ~ 0.4 m. The dark bands are regions of overlapping grooves and the lighter regions contain fewer and less deep grooves. After ~ 300 revolutions the track was completely covered with grooves and the surface roughness was 20–50 nm R_a . No cracks were detected in the ground area. In order to study the shape of the

grooves, grinding was carried out under the same conditions, except that grinding was stopped after one revolution so that no grooves overlapped. An AFM micrograph of eight grooves (Fig. 4a) and the AFM surface profile along the line AB (Fig. 4b) revealed the shape of the grooves produced by individual diamond facets. The groove depths were 26–105 nm with widths up to ~ 2.5 μm . Thus the diamond facets cut V-shaped shallow grooves. The AFM profiles also showed that the groove cross-sections were not symmetrical about

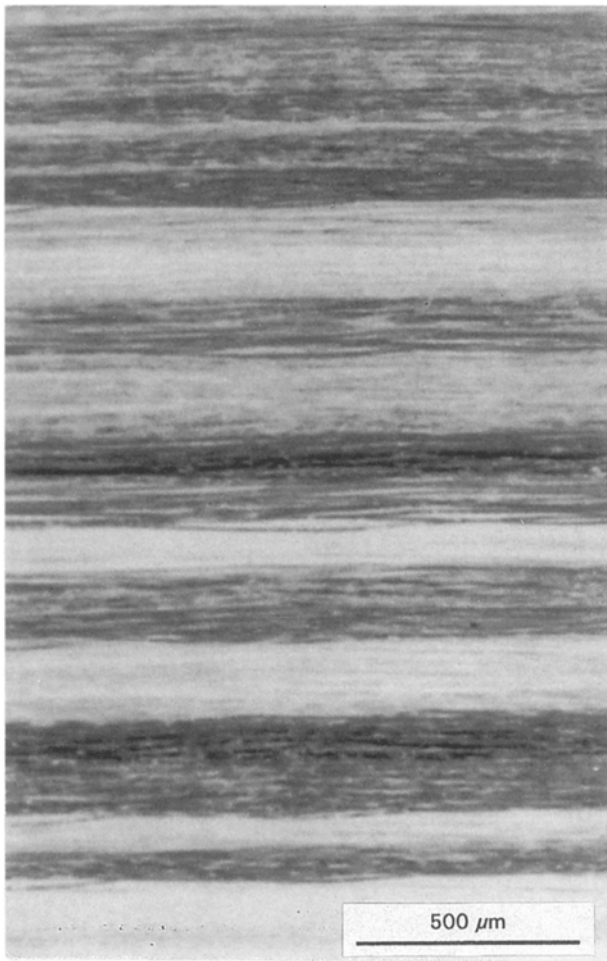


Figure 3 Optical micrograph showing grooves made by a diamond fibre after ten revolutions. $L = 5$ mm, load = 200 g. Ultrasonically cleaned surface.

the surface normal. In Fig. 4b, ridges are visible on the right-hand side of grooves 1–6 and on the left-hand side of grooves 7 and 8. Ridges have been reported in many materials after ductile crack-free grinding and attributed to plastic flow of the material [8, 9, 12]. In the present experiments the ridge heights were less than 27 nm.

In order to determine the groove-cutting mechanism, the surface was sputter coated with gold and examined in the SEM prior to ultrasonic cleaning. After about ten revolutions with 500 g 1 mm fibre the glass surface was covered with fine particulate and filamentary debris around the grooves (Fig. 5a, b). Some wavy filamentary debris many millimetres long (Fig. 6a) and others were coiled with a radius of about $40 \mu\text{m}$ (Fig. 6a, b). The filaments originated from the edge of a groove as shown in Fig. 7a. Initially a thin ribbon of glass is produced at one side of a groove and a filament is formed by fracture along the ribbon as shown in Fig. 7b. Single or multiple fractures can occur (Figs 7b, 8a). Fracture may occur after the groove has been cut, as in Fig. 7a, where a segment of the ribbon remains attached to the groove, but ribbon/filament fracture has occurred on either side of the segment. The observations suggest ductile deformation of the glass introduced residual stresses which sometimes led to fracture of the ribbons. From Fig. 8b

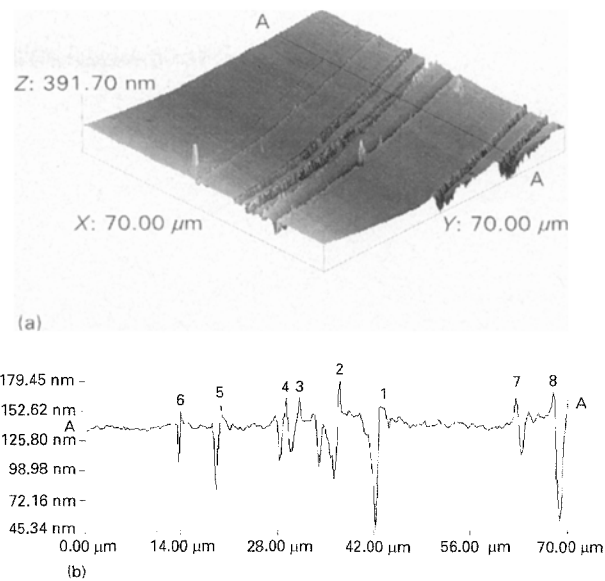


Figure 4 Surface contours obtained by AFM across grooves after one revolution. Ultrasonically cleaned surface. (a) AFM image of $70 \mu\text{m} \times 70 \mu\text{m}$ area. (b) AFM profile of the area in (a) showing eight grooves in $70 \mu\text{m}$ length of track, vertical scale unit 27 nm.

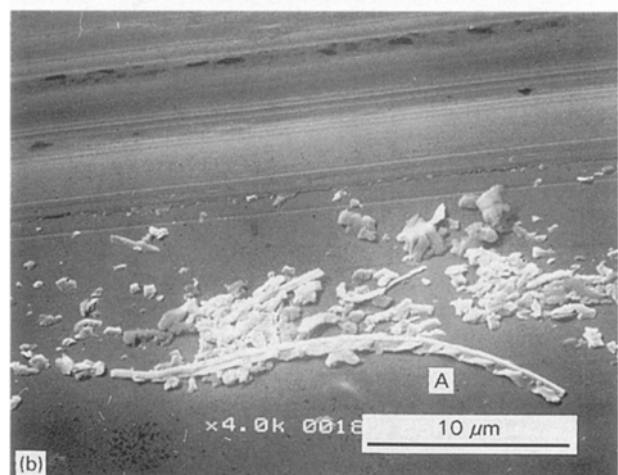
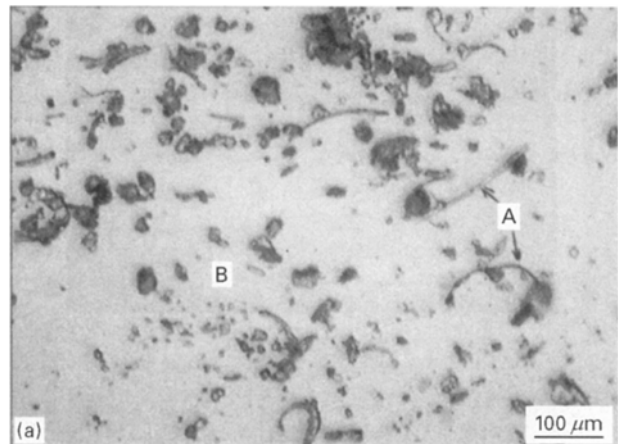


Figure 5 Grinding debris; as-ground surface. (a) Filamentary at A, at particulate B; (b) Filamentary debris showing corrugated deformation at A.

the width of the residual ribbon after the filament has fractured off was about 638 nm at A, and the ribbon thickness at the fracture was about 266 nm . The filaments bent into various shapes as the residual elastic

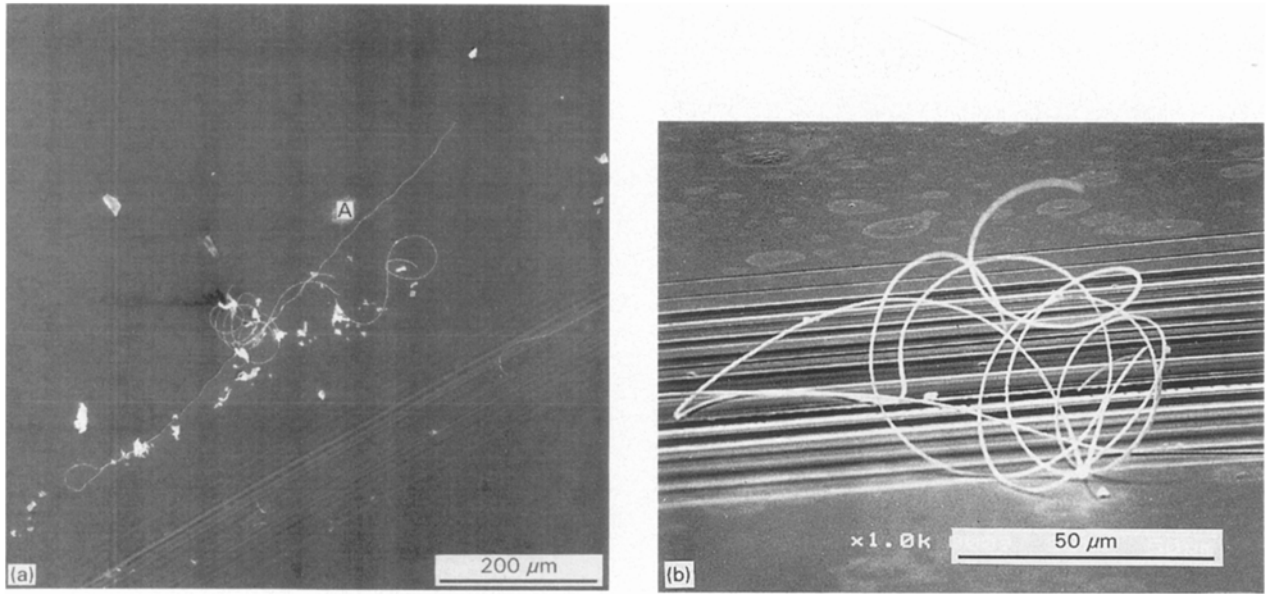


Figure 6 SEM of long filaments: (a) long wavy filament at A; (b) coiled filament on ground track.

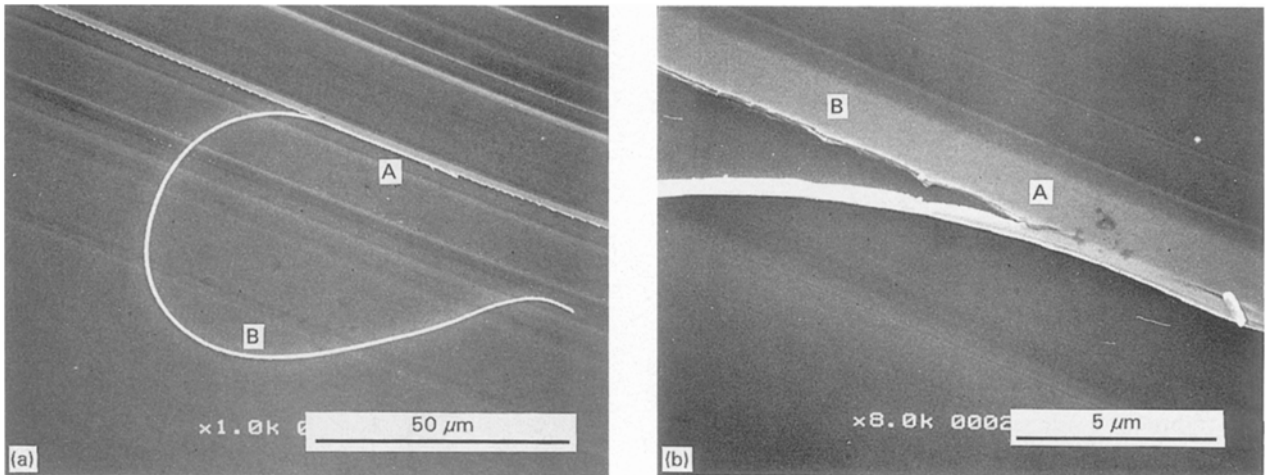


Figure 7 SEM of ribbon and filament. (a) Ribbon at A attached to groove and filament at B fractured from the ribbon. (b) Ribbon/filament fracture at A, groove width at B.

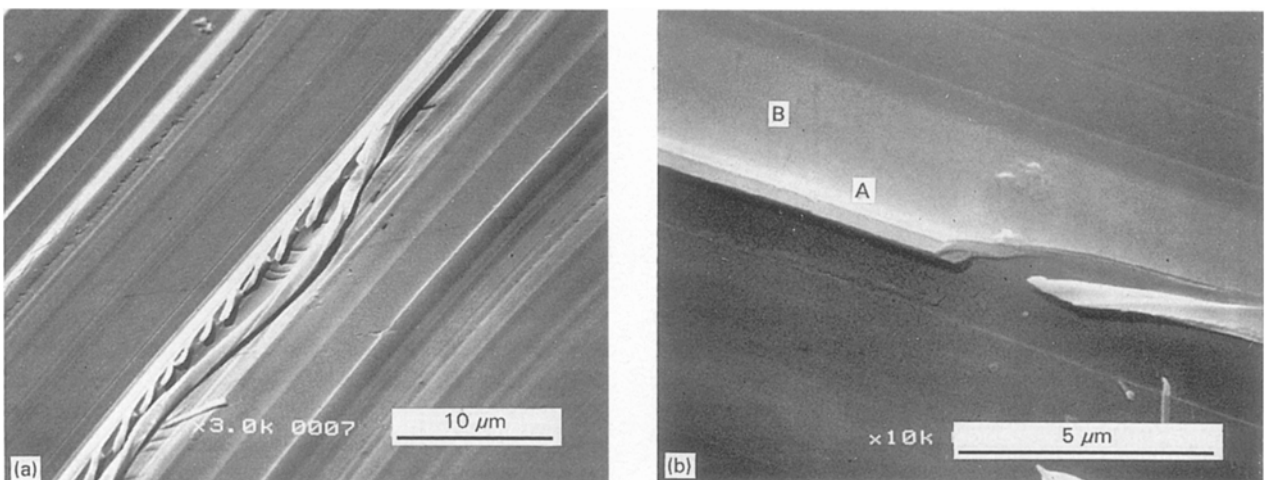


Figure 8 SEM of twisted filament: (a) multiple fractures between the ribbon and the twisted filament; (b) residual ribbon at A, groove at B; (c) twisted filament.

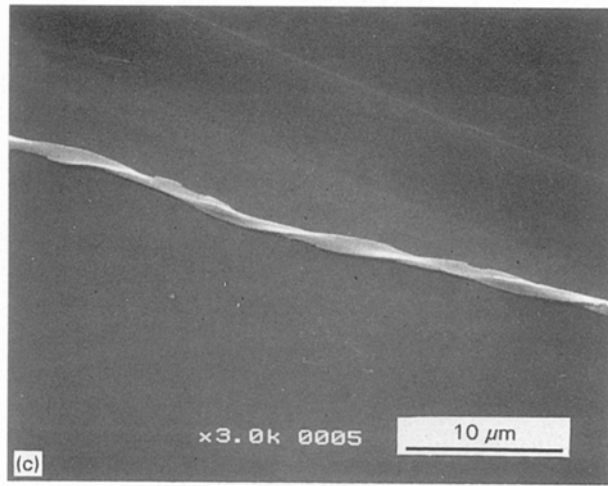


Figure 8 Continued.

stresses were relaxed. A corrugated shape is shown at A in Fig. 5b and a remarkable twisted filament is shown in Fig. 8a and c; the twist is about 19° per micrometre length and the filament remained straight over a length greater than $34 \mu\text{m}$ (Fig. 8c). This regularity of the deformation in the filaments (Figs 5b, 8c) is striking evidence for the generation of a complex but uniform distribution of compressive stresses during the groove-cutting operation. The groove-cutting mechanism appears to be similar to that operating in single-point diamond machining of glass [15]. Extensive grinding had no detectable effect on the diamond facets or the fibres. It is clear that the peaks detected in Fig. 4b at the edge of grooves after ultrasonic cleaning are the residual ribbon lengths.

3.2. Groove geometry and grinding parameters

A section normal to the grinding direction and through a groove and ribbons formed at the groove edges is shown schematically in Fig. 9a. From measurement of the groove profiles in Fig. 4b, the groove angle is typically about 90° . In practice, the groove was seldom symmetrical about the centre-line and many grooves appear to have one face almost 90° and the other face about 3° – 5° to the glass surface, as shown in Fig. 9b. In these cases the glass ribbon and filament only formed at the steeply inclined face above the maximum depth of cut.

The volume of glass removed by grinding under these conditions can be calculated from the volume of the groove, V_G , given by

$$V_G = A_G \cdot L_G \sim \frac{1}{2} w d L_G \quad (1)$$

where A_G is the cross-sectional area of the groove, L_G the length of the groove, and w and d are the width and depth of the groove, respectively. For groove A in Fig. 5b, $w \sim 2.6 \mu\text{m}$, $d \sim 0.105 \mu\text{m}$, giving $V_G \sim 0.14 L_G \mu\text{m}^3$.

If all the glass removed from the groove is present in the ribbon and filament, then the volume of the

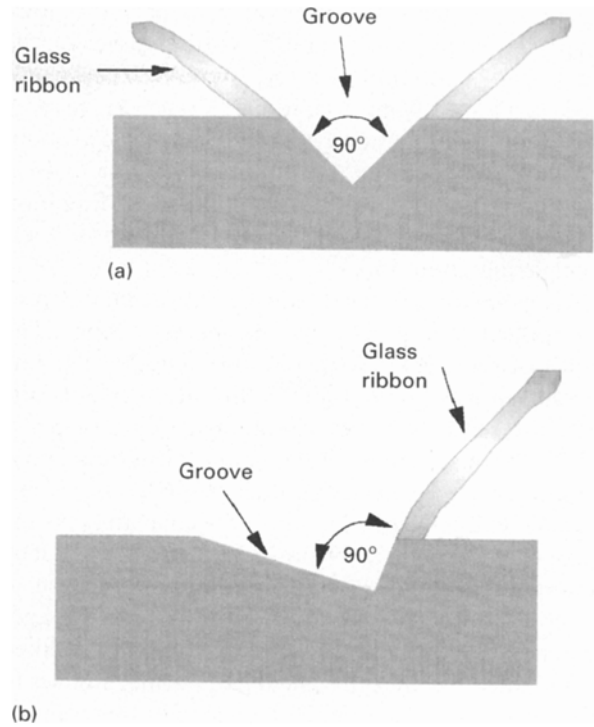


Figure 9 Schematic drawing of the vertical section, normal to the grinding direction, through ground grooves and ribbons: (a) symmetrical groove; (b) asymmetrical groove.

groove, V_G , will equal the volumes of the ribbon plus filament, V_{RF} given by

$$V_{RF} = (A_R + A_F)L_G = t(W_R + W_F)L_G \quad (2)$$

where A_R , A_F and W_R , W_F are the cross-sectional areas and widths of the residual fractured ribbon and filament, respectively, and t is the thickness of ribbon and filament.

From Fig. 8b and c, the total ribbon width before fracture is $W_{RF} = W_R + W_F = \sim 0.354 \mu\text{m} + \sim 1 \mu\text{m} = 1.354 \mu\text{m}$, $t \sim 0.266 \mu\text{m}$, giving the total volume $V_{RF} \sim 0.36 L_G \mu\text{m}^3$. The difference in the values for V_G and V_{RF} reflect the fact that the filaments were not obtained from the measured grooves in the present experiments and the very small groove dimensions were particularly difficult to measure.

It is important to know the glass-removal rate under ductile grinding conditions. This is given by

$$R^* = V_G N_G v \text{ mm}^3 \text{ s}^{-1} \quad (3)$$

where N_G is the number of grooves, and v the rotations per second of the glass disc. For the fibre case, and assuming each diamond pyramid on the fibre surface cuts a groove, as in Fig. 2

$$N_G = L_F N_F / x \quad (4)$$

where x is the spacing between the pyramids in the axial direction, N_F the number of fibres and L_F the length of fibre (L_F is equivalent to the wheel width in the grinding literature). If N_G is normalized with respect to the fibre length, L_F , then using Equation 1

$$R = w d L_G N_F v / 2x \text{ mm}^2 \text{ s}^{-1} \quad (5)$$

where R is the glass removal rate per unit fibre length, $L_G = 2\pi r$, $r \sim 19$ mm, the cutting radius on the glass, per revolution. In the present experiments, $\frac{1}{2}wd \sim 0.14 \mu\text{m}^2$ from Equation 1, $v = 0.41 \text{ rev s}^{-1}$, $N_F = 1$, and the diamond pyramids were spaced about $5 \mu\text{m}$ apart, giving a maximum value for $x \sim 5 \times 10^{-3} \text{ mm}$ ($\sim 200 \text{ mm}^{-1}$). Substitution in Equation 5 gives a maximum value of $R \sim 10^{-3} \text{ mm}^2 \text{ s}^{-1}$ for a single diamond fibre.

An estimate can be made of the normal stress, σ_N applied to the glass by the diamond fibre. The width of the track (along the fibre length) after one revolution was about 1 mm, with only $\sim 10\%$ of the area covered by grooves. Assuming a depth of cut of $0.105 \mu\text{m}$, the circumferential contact length is about $6.5 \mu\text{m}$, giving an area of contact of $\sim 6.5 \times 10^{-10} \text{ m}^2$. The 200 g (2 N) applied load produced a stress on the glass of about $= 3100 \text{ N mm}^{-2}$ compared with 3600 N mm^{-2} for the yield stress of soda glass. Because, in the contact area, it is not known how many facets are present and their contact areas, σ_N can only be taken as an indication that the calculated normal stresses in the present tests were much higher than the nominal values reported for grinding wheels ($\sim 30 \text{ N mm}^{-2}$) under ductile grinding conditions.

4. Discussion

It is difficult to compare directly the present results for the fibre with ductile grinding wheel data. For example, a much higher calculated normal stress of 3100 N mm^{-2} was obtained for diamond fibre surfaces compared with the normal stresses reported for diamond wheels of $\sim 3\text{--}30 \text{ N mm}^{-2}$ [9, 12]. The latter may be misleading, because the yield stress of glass is closer to the calculated fibre normal stress value. The discrepancy may be caused by the fact that in a typical vitrified natural diamond grinding wheel, with 75% by volume diamond particles, 18.75% bonds and 6.25% voids, the load may actually be carried by individual particles, while the stress is calculated on the contact area of the wheel. Thus the true stress on the glass in the grinding wheel case is probably much higher.

The surfaces of CVD diamond films usually have a strong texture [14], with the dominant crystal facets (111), (100) and (110) intersecting along $\langle 110 \rangle$ and $\langle 100 \rangle$ edge directions. For a typical $\langle 100 \rangle$ textured deposit, a pyramidal diamond point and its associated facets formed by a columnar diamond grain at the fibre surface is shown at A in Fig. 1b and the facet geometry is shown schematically in Fig. 10a. The pyramid surface is composed of inclined (111) planes which intersect along $\langle 110 \rangle$ directions. The shape of the octahedral facets looking in the [100] direction is shown in Fig. 10b; the $\langle 110 \rangle$ edges are at 90° . The shape of the grooves in Fig. 4b can be explained by assuming a [100] grinding direction and a groove cut by the $\langle 110 \rangle$ edges. Similarly grooves may be cut by $\langle 100 \rangle$ edges associated with cube faces. In the present experiments, the diamond facets and edges on the fibre surface acted as single-point diamonds for cutting grooves in glass.

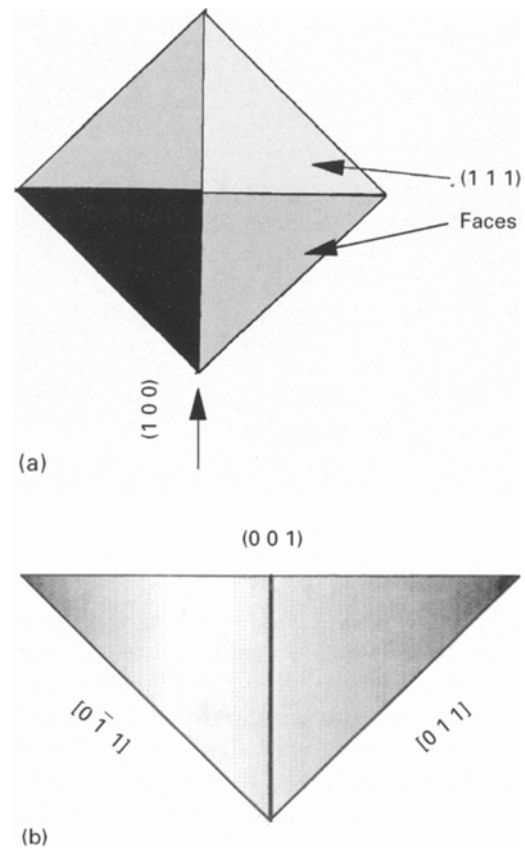


Figure 10 Schematic drawings of diamond fibre facets: (a) plan view; (b) view in plane normal to grinding direction.

The shape of the grooves cut by the grinding wheel diamond grit are generally deeper with groove angles of about 140° [8] and with a $5 \mu\text{m}$ diameter grit the measured grit surface area density was reported to be about $50 \text{ particles mm}^{-2}$ [15]. A diamond fibre surface is 100% diamond, with $\sim 90^\circ$ groove angle, and an effective diamond pyramid spacing of $\sim 5 \mu\text{m}$, giving $\sim 10^4$ cutting points mm^{-2} . The important parameters for commercial ductile grinding [8, 10, 11] are diamond particle size and volume fraction, normal force on the wheel, feed per wheel revolution and depth of cut, with the ductile mode particularly favoured by a small grit size. A small grit size and high volume fraction is recommended for minimum grinding time in the ductile grinding mode [11]. The fibre surface with a combination of a high density of very small cutting edges should favour the ductile grinding mode and a high rate of material removal.

It is worth noting that ductile grinding on glass has been obtained at much greater speeds and depth of cut than used in the present tests, e.g. using a 200 mm diamond wheel rotating at 360 r.p.m. (4.1 m s^{-1}), in-feed rate of 0.46 m s^{-1} , depth of cut $1\text{--}2.5 \mu\text{m}$ [8, 9, 10]. A simple measure of the potential for higher cutting rates with diamond fibres may be obtained by considering an increase in the depth of cut, d , and the number of fibres, N_F . For the geometry of Fig. 9b, $d = 0.105 \mu\text{m}$, Equation 1. If the number of fibres can be increased to 100, i.e. the single-fibre specimen is replaced by a $5 \text{ mm} \times 10 \text{ mm}$ disc, then from Equation 5, a predicted removal rate of $R \sim 10^{-1} \text{ mm}^2 \text{ s}^{-1}$ is obtained, which is at the top end of the rate range

reported for micro-grinding of 10^{-4} – 10^{-1} mm²s⁻¹ [11]. The obvious step is to place the fibres on the circumference of a grinding wheel. A typical 200 mm diameter wheel could accommodate ~6370 fibres. With only 10% of the facets actively cutting and only 10% of the fibres in contact with the surface, a high rate of material removal under ductile grinding conditions would be expected.

The present experiments have shown that diamond fibres can be used to grind glass under ductile flow conditions without the brittle surface cracks associated with conventional abrasive grinding of glass. The grinding mechanism appears similar to that reported for single-point diamond machining and micro-grinding carried out in specially designed rigid machines [9, 11, 13, 16, 17], compared with the simple pin-on-disc machine used in the present experiments. This suggests that the ductile grinding conditions may be less critical with diamond fibres. This is supported by the ease with which very low surface roughness values can be obtained on alumina by diamond fibre grinding [18]. The polishing stage following grinding and lapping [19] is known to be very time consuming and expensive for ceramic and optical materials and silicon [10]. Recent studies have indicated that the final stage of polishing of optical lenses may be substantially reduced or omitted completely by ultra-precision single-point or line contact diamond grinding, [9, 16, 20]. This is an important development and the above results suggest diamond fibres may be uniquely suited for precision ductile grinding of glass and optical ceramics.

5. Conclusion

Single chemical vapour deposited diamond fibres have been used to grind soda glass. The high density of small diamond surface facets and diamond edges led to ductile grinding without surface cracking. The grinding mechanism, involving the formation of nanoscale glass ribbon swarf by flow of the glass adjacent to the grinding grooves, was similar to that found in single-point diamond machining. The use of multiple fibres is predicted to produce high material removal rates in the ductile grinding mode and the fibres have potential in ultra-precision ductile grinding of glass and optical ceramics.

Acknowledgements

The authors thank P. Shore (Cranfield Precision Engineering), J. P. Gallemaers and M. Wilson (Diamant Boart S A) for helpful discussions, B. Mortimer and C. M. Ward-Close, DRA(F) for use of their facilities and equipment, and M. N. R. Ashfold, School of Chemistry, G. Allen, Interface Analysis Centre, and

J. W. Steeds, Physics Department, for supporting the diamond research programme in the University. A.F., E.D.M. and G.M. thank EPSRC, and P.G.P. thanks DRA(F) for financial support.

References

1. J. L. METZGER, "Superabrasive Grinding" (Butterworths, 1986).
2. R. I. KING and R. S. HAHN (eds), "Handbook of Modern Grinding Technology", (1986) (Chapman and Hall, London 1988).
3. P. G. PARTRIDGE, P. W. MAY and M. N. R. ASHFOLD, *Mater. Sci. Technol.* **10** (1994) 177.
4. B. LUX and R. HAUBNER, *Philos. Trans. R. Soc.* **A342** (1993) 297.
5. E. D. NICHOLSON, T. W. BAKER, S. A. REDMAN, E. KALAUGLER, K. N. ROSSER, N. M. EVERITT, M. N. R. ASHFOLD and P. G. PARTRIDGE, *Diamond Rel. Mater.* (1996) 'Young's Modulus of Diamond-coated Fibres and Wires' Vol. 5, No. 6-8 pp. 658–63.
6. P. G. PARTRIDGE, P. W. MAY, C. A. REGO and M. N. R. ASHFOLD, *Mater. Sci. Technol.* **10** (1994) 505.
7. M. N. R. ASHFOLD, P. W. MAY, E. D. NICHOLSON, P. G. PARTRIDGE, G. MEADEN, A. WISBEY and M. J. WOOD, in "3rd International Conference on the Applications of Diamond Films and Related Materials", August 1995, Editors A. Feldman, Y. Tzeng, W. A. Yarborough, M. Yoshikawa, M. Murakawa, US Government Printing Office, Washington. Gaithersburg, National Institute of Standards and Technology Special Pub. 885 (1995) 529.
8. M. HUERTA and S. MALKIN, *Trans. ASME J. Eng. Ind.* Vol. 98 (1976) 459.
9. Y. NAMBA and M. ABE, *Ann. CIRP* **42** (1993) 417.
10. Z. ZHONG and V. C. VENKATESH, *J. Mater. Process. Technol.* **44** (1994) 179.
11. T. G. BIFANO, T. A. DOW and R. O. SCATTERGOOD, *Trans. ASME J. Eng. Ind.* **113** (1991) 184.
12. K. KITAJIMA, G. O. CAI, N. KUMAGAI, Y. TANAKA and H. W. ZHENG, *Ann. CIRP* **41** (1992) 367.
13. Y. NAMBA, Y. YAMADA, A. TSUBOI and K. UNNO, *ibid.* **41** (1992) 347.
14. Y. SATO and M. KAMO, *Surf. Coat. Technol.* **39/40** (1989) 183.
15. K. E. PUTTICK, M. R. RUDMAN, K. J. SMITH, A. FRANKS and K. LINDSEY, *Proc. R. Soc. A* **426** (1989) 19.
16. J. E. MAYER and G.-P. FANG, "Advancement of Intelligent Production" (Japan Society for Precision Engineering, (1994) pp. 285.
17. W. KONIG and V. SINHOFF, *SPIE* **1780** (1992) 778.
18. P. G. PARTRIDGE, A. J. FOOKES, T. PEARCE and G. MEADEN, Nanoscale surface grinding of ceramics using diamond fibres, June 1995, University of Bristol.
19. N. B. KIRK and J. V. WOOD, *Br. Ceram. Trans.* **93** (1994) 2530.
20. J.-D. KIM and C.-H. MOON, in "3rd International Conference on the Applications of Diamond Films and Related Materials", August 1995, Editors A. Feldman, Y. Tzeng, W. A. Yarborough, M. Yoshikawa, M. Murakawa, US Government Printing Office, Washington. Gaithersburg National Institute of Standards and Technology Special Pub. 885 (1995) p. 213.

Received 6 February
and accepted 18 March 1996